Evaluation of disturbance induced on soft offshore sediments by two types of gravity piston coring techniques

Tommasi P.[a,*], Avalle A.[a,1], Budillon F.[b], Romeo R.[c], Caburlotto A.[c], Conforti A.[d], Di Martino G.[b], Pagliaroli A.[e], Magagnoli M.[f], Urgeles R.[g], Llopart J.[g], Camerlenghi A.[c]

[a] IGAG-CNR, Istituto di Geologia Ambientale e Geo-Ingegneria, Area della Ricerca di Roma1, Via Salaria km 29,300, 00017 Monterotondo Stazione (RM), Italy. paolo.tommasi@cnr.it

[b] ISMAR-CNR- Istituto per le Scienze Marine, Calata Porta di Massa, 80133 Napoli, Italy

[c] OGS, Borgo Grotta Gigante 42/C, 34010 Sgonico (TS), Italy

[d] IAS-CNR Istituto per l'impatto Antropico e la Sostenibilità dell'Ambiente Marino, Loc. Sa Mardini, Torregrande, 09072 Oristano, Italy

[e] Università degli Studi "G. d'Annunzio" di Chieti Pescara, viale Pindaro 42, 65129 Pescara, Italy

[f] Carmacoring S.r.l., Via del Colle, 27, 40068 San Lazzaro di Savena (BO), Italy

[g] Departament de Geociències Marines, Institut de Ciències del Mar (CSIC), Barcelona, Spain

*Corresponding Author, Tel. +39-06-44585005; paolo.tommasi@uniroma1.it
alessandra.avalle@gmail.com (A. Avalle), francesca.budillon@cnr.it (F. Budillon), rromeo@inogs.it (R. Romeo), acaburlotto@inogs.it (A. Caburlotto), alessandro.conforti@cnr.it (A. Conforti), gabriella.dimartino@cnr.it (G. Di Martino), alessandro.pagliaroli@unich.it (A. Pagliaroli), massimo@carmacoring.it (M. Magagnoli), urgeles@icm.csic.es (R. Urgeles), acamerlenghi@inogs.it (A. Camerlenghi)

Keywords: sample disturbance, geotechnical properties, laboratory tests, seabed sampling, magnetic susceptibility

[1] Present affiliation: Università Roma Tre, Via Vito Volterra 62, 00146 Roma, Italy

Highlights

- Comparison of disturbance induced by a conventional free fall piston corer and a modified piston corer
- Sampling of pelitic sediments with a prevailing non-clayey fraction with interspersed tephra horizons
- Analysis of accelerometer, magnetic susceptibility logs and laboratory geotechnical properties
- Reduced core shortening in modified-piston-corer samples revealed by magnetic susceptibility logs,
- Higher small-strain shear modulus, G_0, in modified-piston-corer specimens revealed by cyclic shear tests
- Equivocal response of oedometer compression tests

Abstract

Sample disturbance is still a key issue in offshore investigations, especially when logistic and financial limitations do not allow the use of drilling equipment. This paper focuses on the comparison between the disturbance induced by a conventional free-fall piston corer (FF) and a modified piston corer (AD) equipped with a velocity control (Angel Descent method). Twin core samples were retrieved in two successions of pelitic sediments with a prevailing non-clayey fraction and a non-negligible sandy fraction. Comparison was based on different acquisition, physical and mechanical parameters ranging from accelerometer data to magnetic susceptibility logs and geotechnical parameters from laboratory investigations, including oedometer compression tests and cyclic simple shear tests. Accelerometer data highlighted the sharp reduction in velocity obtained for AD samples. Magnetic susceptibility logs, characterized by a pattern of peaks induced by several volcaniclastic levels present in the succession, indicated that the AD method significantly reduces core shortening. Among geotechnical investigations, cyclic shear tests provided small-strain shear moduli always higher in AD samples, whilst the response of oedometer compression tests was equivocal. In fact, methods for assessing sample disturbance have demonstrated to bear limited effectiveness when applied to soils with relatively low clay content and significant overconsolidation as it is the case of the studied sediments.

1. Introduction

Many geotechnical, geological and geophysical analyses for both research and design purposes, require the knowledge of physical and mechanical properties, e.g. undrained shear strength, strength parameters in effective stresses, stiffness and damping parameters. These parameters are affected by soil disturbance induced by the sampling procedure, which is particularly significant in most offshore projects. Lunne et al. (2006) state that block sampling is by far the least invasive method, and that tube sampling unavoidably induces disturbance that alters the sediment structure (including cementation) with negative fallout on a number of geotechnical test results. A further consequence of disturbance induced by gravity and piston coring is core shortening/elongation, which alters the actual depth of geological horizons used for calculating sedimentation rates or reconstructing sub-bottom stratigraphy. Nevertheless, very often deep water investigations are conducted through vessel-operated gravity/piston corers.

Sample depths over 0.7 meter below the sea floor (i.e., that reached by spade box corers) require borehole block sampling and hence drilling devices operated from stable structures (pontoons, barge rigs) or drilling vessels. The former can be used when the water depth is shallow, whilst the latter are too expensive for many research projects.

In this paper we present and discuss the results of a coring campaign conducted with a standard piston gravity corer and a gravity piston-corer specifically designed to minimize sediment disturbance (Magagnoli, 2017). The aim of this study is to evaluate the performance of the two devices in terms of disturbance by comparing three characteristics of the retrieved core samples: shortening, behavior in oedometer compression and cyclic simple shear tests.

2. Previous Studies

2.1 Quantitative assessment of disturbance

Using International Ocean Discovery Program (IODP) cores, Jutzler et al. (2014) identify various types of disturbance resulting from: (i) shear deformation of sediment against the core barrel; (ii) sand basal flow-in; (iii) fall-in; (iv) sediment loss through core catchers; and (v) formation of new structures during core recovery and on-deck transport. Some of these disturbances, such as flow-in or fall-in, result in samples obviously not ~~fit~~ suitable for geotechnical testing. For other disturbances, such as shear deformation, sample suitability may depend on the amount of disturbance. The degree of disturbance of an offshore sample has been estimated through different qualitative and quantitative methods based on the analysis of structural, physical, and geotechnical properties of the sediment at different scales.

A routine investigation at the sample scale is the analysis of the curvature of sediment laminae through X–ray digital scans (initially proposed by Jamiolkovski et al., 1985), which provides qualitative information on the extent and intensity of deformation suffered by the sample annulus subjected to the dragging action of the tube wall. Also in-situ measurements have been compared to laboratory measurements to quantify vertical disturbances in piston cores. Garziglia (2010) correlates p-wave velocity measurements performed on the core and those measured in-situ through a sonic cone near the sample location, to correct the depth of the cored sediment.

An interesting quantitative parameter at relatively large scale is the difference between the sediment thickness that was actually penetrated and the core length. This parameter, generally referred as shortening, can be estimated by comparing penetration and sample length. In the marine environment the assessment of the former datum is not trivial; it can be inferred for instance, from accelerometer data or the sediment-coated length of the external tube wall.

A relative assessment of shortening induced by different sampling devices can be conducted by comparing logs of properties, such as magnetic susceptibility (see e.g. Jeanjean et al. 2005), reflectance (Govin et al., 2016), or carbonate content, provided that markers can be identified with sufficient frequency along the core. In this respect magnetic susceptibility not only allows detection of core shortening but its use in stratigraphic reconstruction is spoiled by shortening itself (Shimono et al., 2014).

In gas-bearing sediments further disturbance is produced by the variation in the state of effective stress and temperature experienced by the sediment after sampling with conventional techniques (Dück et al., 2019). To overcome these difficulties, special pressure samplers (e.g. Lee et al., 2013) or freeze corers (see e.g. Dück et al., 2019) have been utilized to recovery samples for sediment characterization with a limited geotechnical target. Otherwise, to avoid influence of disturbance on sampling for geotechnical purposes, in situ geotechnical testing has been preferred (e.g. Taleb et al., 2018).

The earliest disturbance index based on the geotechnical behavior is the volumetric strain experienced during recompression, i.e. up to the in situ effective stress (Andresen and Kolstad, 1979). This index has been successively replaced by Lunne et al. (1997) with the variation of void ratio during reconsolidation normalized to its initial value ($\Delta e / e_0$). Successively Lunne et al. (2006) warned against using this parameter for ~~soils~~ sediments outside a specified range of plasticity index, water content, overconsolidation ratio and sampling depth.

Since then, analysis of the effects of disturbance has been progressively refined based on evaluation of the degree of structure obliteration and volume changes. The assessment of structure perturbation applies to soft clays (Hight and Leroueil, 2003 and Ladd and DeGroot, 2003). In this respect, Lunne et al. (2008) have illustrated the effects of different sampling methods on the compressibility and consolidation behaviour of Norwegian offshore soft clays, which is affected by the structure change. On this basis, Lunne et al. (2008) highlight the effectiveness of Constant Rate of Strain (CRS) oedometer tests, especially through plots of constrained modulus M versus the vertical effective stress σ'_v in the linear plane. In this regard, Karlsrud and Hernandez-Martinez (2013) linked the four quality classes proposed by Lunne et al. (1997) to the ratio between the maximum (M_0) and the minimum (M_L) constrained moduli determined before and after the apparent pre-consolidation stress, respectively (hereafter indicated as M–ratio). **Tab. 1** shows the quality classes proposed by Lunne et al. (1997) and Karlsrud and Hernandez-Martinez (2013), based on the values of $\Delta e / e_0$ and M_0 / M_L, respectively.

A combination of the two occurs in the so-called intermediate soils (Lukas 2018), i.e. those with prevailing non-clayey fraction and low plasticity. In this sense Krage et al. (2015) stressed limitations of the procedures for assessing sampling disturbance proposed by Lunne et al. (1997, 2006, 2008) ("clay-based" procedures) when applied to sediments with a significant amount of grain-size fractions coarser than clay, where partial drained conditions could occur during sampling.

Lunne et al. (2006) observe that, besides oedometer compression tests, disturbance affects especially consolidated undrained tests, in particular by reducing undrained strength and initial stiffness and by increasing strain at failure.

Dynamic properties were used by Tan et al. (2002), Landon et al. (2007) and Donohue and Long (2010) to assess disturbance. In the first two studies, shear wave velocity was measured with the bender elements technique on low-OCR silty clays. In the latter, shear wave velocity was measured in combination with suction on relatively soft silty clays and clayey silts. In all cases tube samplers of various types were used during onshore borehole investigations.

2.2 Sampling techniques

Amongst gravity-driven vessel-operated devices capable of sampling well below the first meter of sediment, piston gravity coring allows recovery of longer, generally less-disturbed and relatively complete cores (Gallmetzer et al., 2016). However, a prerequisite is that the sampling system is modified to reduce the disturbance that is usually induced by the conventional method, without compromising core recovery.

Improvements to the piston coring method have been proposed by different authors to meet specific requirements of core analyses, and are thoroughly described by Lunne and Long (2006). Except for the Giant and Jumbo piston corers, or the HPC-APC piston corer operated by the IODP cruises, however, which operate from large vessels, the most effective improvement to the traditional piston coring was probably introduced ~~in~~

by the STACOR sampler (Montarges et al., 1983), where the piston is fixed to the seabed rather than be connected to the vessel, as in the standard piston corers. Lunne and Long (2006) notice that STACOR logistics are complex, especially with reference to deployment time. Improvements were also recently brought to the giant Calypso corer operating from the R/V Marion Dufresne, especially by reducing cable elasticity and optimizing the corer setup through a software for simulation of coring dynamics and sensors for monitoring coring parameters (Govin et al., 2016).

Also Gallmetzer et al. (2016) have recently designed a piston corer for retrieving large-diameter cores from a small boat, which allowed negligible core shortening. This achievement results from the combined action of the piston, the large diameter and a static loading system that allows slow penetration. Unfortunately the use of this device is restricted to shallow water depths and yields short penetration.

Samples with a reduced degree of disturbance have also been taken in soft pelitic sediments (silty clay) through a 90 mm diameter vibrocorer operated without vibration and free-fall from the water-sediment interface (Lanzo et al., 2009). The use of this device is restricted to soft sediments at maximum water depths of 300 m and allows moderate penetration (4-5 m). Samples obtained with this device showed a quality index $\Delta e/e_0$ between 0.04 and 1.

3. Methods

3.1 Sampling

Seafloor sampling was performed in September 2014 during the SAOS (Stability Assessment of an Open Slope) cruise onboard R/V Urania (CNR) within the national research project RITMARE. The cruise was jointly organized by the IAMC (now ISMAR) and IGAG institutes of the National Research Council (CNR) and the National Institute of Oceanography and Applied Geophysics (OGS).

The objective of the SAOS Cruise was to collect geological, geophysical and geotechnical data for the study of the Licosa submarine landslide, located on the upper slope off the Cilento coast in the South Tyrrhenian Sea (Southeastern Italy) (Fig. 1; see also Bellonia et al., 2008; Sammartini et al., 2018).

At three of the ten coring locations during the SAOS cruise, the coring operations were duplicated using a standard piston corer and a Carmacoring piston corer employing the Angel Descent® method described in Magagnoli (2017).

Pairs of replicate cores were collected at two sites. One pair at Site A, on an intra-slope basin west of the Paestum Basin in 673 m water depth (Core A; Fig. 1). Two pairs of cores at Site B, located just up-slope of the Licosa Landslide crown scarp in the un-failed sedimentary section in about 250 m water depth (cores B2 and B3; Fig. 1). Hereafter the standard and the modified coring methods will be indicated with the acronyms FF (Free-Fall) and AD (Angel Descent®), respectively. The FF and AD coring methods employed the same piston coring tool, provided with PVC liners 100 mm in diameter (outer) and a cutting shoe with an angle of 10°. This angle ensures an acceptable disturbance, given that the area ratio is about 17% (Andresen 1981), and easily cuts the thin gravelly horizons interspersed in the finer sediment. The corer was operated with a polyester-kevlar cable, which has a negligible weight in marine water (Shilling et al., 1988). The acquisition parameters are summarized in **table 2**. The AD coring method, described in detail by Magagnoli (2017), is characterized by null free-fall length and wire slack and variable core speed during penetration. To overcome increasing lateral resistance along the corer wall, the corer speed is low at the beginning of penetration and successively increases as penetration proceeds. The speed control is actuated through an especially designed winch (provided with a brake) connected to the main cable, just above the trigger. The hook of the winch wire is connected to the eyebolt of the corer head. The initial penetration speed of the corer is adjusted according to the resistance to penetration of the sediment by setting up the winch brake before coring (the softer the sediment, the tighter the winch brakes are). With this method, the elastic rebound force applied on the cable by the release of the corer weight is strongly reduced (Skinner and McCave, 2003).

At both sites accurate positioning of the vessel, provided by an Omnistar-Fugro 12-channel differential GPS navigation system, allowed coring operations to be replicated within two meters error distance, so that the coring locations can be assumed to be identical for the FF and AD cores.

In order to assess lateral continuity, geometry and thickness of the horizons at the coring sites, high-resolution reflection seismic profiles were collected and carefully examined before undertaking coring operations. Seismic profiles were obtained by means of a Datasonic CHIRP III sub-bottom profiler, hull-mounted aboard the R/V Urania and generating a FM sweep pulse, as a source signal, with a frequency band of 2-7 kHz. The vertical resolution of the seismic record immediately below the seabed is about 0.7 ms (1 m) at site A and about 0.6 ms (0.9 m) at site B; penetration is higher than 50 ms (720 m) in both cases. The conversion from milliseconds to meters as well as the depth scale in Fig. 2 have been obtained by using an average value of the longitudinal wave velocity of the water column equal to 1520 m/s, based on sound velocity probe measurements.

At site A (deep water intraslope basin), the penetrated sediments consist of a horizontally bedded succession of fine-grained hemipelagics, thin tephra layers (1 to 10 mm-thick) and turbidites (**fig. 2A**). A high-amplitude and laterally continuous reflector occurs at about 9 ms two-way travel time reflecting a thicker and coarser-grained turbidite. It was sampled only at the bottom of the core A-FF, which penetrated further than core A-AD (**fig. 2**).

At site B the two cores (B2 and B3) were collected from an upper slope succession formed by alternating layers of fine bioclastics, sandy-clayey silts and tephra, with thicknesses varying from few centimetres to few tens of centimetres (Iorio et al., 2014). Bedding is sub-parallel and laterally continuous dipping less than 4° following the general dip of the upper slope (**figs. 2B and 2C**).

During coring operations, the following parameters were measured: vertical accelerations at corer head, cable length, winch speed and winch load. Corer setup and coring results are reported in **table 2**.

Penetration was inferred from the distance between the corer tip and the highest point where mud was stuck on the barrel surface. A quantitative estimate of penetration was attempted by integrating acceleration data with the winch velocity at core release as integration constant (Heffler, 1991). However, these values were discarded because the resulting penetration was systematically shorter than that estimated visually (similarly to observations reported by Bourillet et al., 2007).

The retrieved cores were cut into 1 m-long sections, sealed with Parafilm® and maintained at 4°C during both the cruise and the laboratory testing period.

3.2 Physical and geotechnical laboratory investigations

Laboratory investigations consisted ~~in~~ of a) quasi-continuous measurement of magnetic susceptibility (MS); b) high-definition X-ray scanning of cores; c) oedometer compression and d) cyclic shear tests on twin specimens from replicated cores.

Magnetic Suceptibility was measured onboard on the core sections with 20 mm spacing using a Bartington Instrument, MS2C loop sensor, 125 mm in diameter.

High-resolution X-ray Computed Tomography (CT) scans were performed at MARUM, University of Bremen (Germany). For the purpose of the investigation two orthogonal X-ray scans were performed with a mobile GE ProSpeed SX Power CT Scanner. This system offers a highly efficient slip-ring scanner for medical requirements converted to sedimentological purposes. 81 images were obtained in DICOM format (Digital Imaging and Communications in Medicine) post-processed with MicroDicom free viewer.

Oedometer compression tests were conducted with both the incremental loading procedure (ILOC) and the constant rate of strain procedure (CRS). Oedometer IL tests were performed at OGS in Trieste (Italy), whilst CRS tests were performed at Institut de Ciències del Mar (CSIC) in Barcelona (Spain) using a GDS CRS-type cell equipped with two advanced 2MPa pressure/volume controllers and a 50 kN load frame. Samples for all oedometer compression tests had an initial specimen height of 20 mm and an initial sample diameter of 50 mm.

Strain-controlled cyclic simple shear tests were conducted at the University of Rome "La Sapienza", Italy, through the DSDSS device (D'Elia et al., 2003; Lanzo et al., 2009) based on the prototype of the University of California at Los Angeles (Doroudian &Vucetic, 1995). The peculiarity of the DSDSS device (Double Specimen Direct Simple Shear Test) consists in the simultaneous shearing of two specimens of the same soil (**fig. 3**). Due to its specific configuration and to the large stiffness of the device components, all the problems associated with false deformations and system compliance are negligible, thus enabling the measurement of soil properties even at very small strains (≈0.0004%).

At the completion of primary consolidation under the specified vertical load σ'_v, the specimens are subjected to several steps of cyclic shearing. Cyclic strain is manually applied following a sinusoidal path with a frequency usually ranging from 0.1 to 0.3 Hz. The strain amplitude γ_c of the shear cycle is increased at steps consisting of 10 cycles. For each cycle, the equivalent shear modulus (G_{eq}) and damping ratio (D) are defined (**fig. 4**), and average values of G_{eq} and D are calculated for each step.

Identification tests were conducted on almost all specimens following ASTM procedures. Grain density was determined with a helium pycnometer, Atterberg limits were determined through standard procedures (fall cone measures were carried out on CRS specimens but are not reported), and grain size was determined through the sieve analysis and sedimentation method.

4. Assessment of sampling disturbance

To assess disturbance, different aspects were investigated through in situ measurements and laboratory investigations:

a) core shortening, evaluated by comparing quasi-continuous logs of magnetic susceptibility (see e.g., Jeanjean et al., 2005);
b) dynamic parameters during corer penetration;
c) behaviour in oedometer compression and under cyclic simple shearing of selected samples retrieved at approximately the same location within the sedimentary sequence.

At Site A all aspects were investigated whilst at site B only core shortening and corer dynamics were analyzed.

4.1 Coring dynamics

Acceleration and velocity histories at the corer head for the three twin coring operations are plotted in **figure 5**. Recording of AD coring at site B2 was interrupted before completion of penetration. For AD corings penetration virtually coincides with the core release, whilst in FF cores determination is not immediate and can be inferred from the analysis of acceleration histories (Heffler., 1991; Villinger et al., 1999; Bourillet et al., 2007). Velocity was calculated by integrating acceleration with an initial velocity equal to that measured at the winch (0.26, 0.56 and 0.2 m s^{-1} for A, B2 and B3 cores respectively). All plots highlight that FF coring penetrate at a maximum velocity that is from 1.5 to more than 4 times higher than the AD corings. In AD corings velocity remains low even after penetration and in the phase of upward movement, which in the FF corings instead occurs with high acceleration and velocity (5 – 30 m s^{-2} and 2 – 5 m s^{-1}, respectively).

4.3 Core shortening

Core shortening has been a key issue in sediment sampling since the middle of the past century (Emery and Dietz, 1941). Shortening is largely attributed to the plugging of the bottom part of the core which forces the in situ sediment to flow aside outside the coring tube as the corer penetrates, thus preventing further recovery (see e.g. Chaney and Almagor, 2015). However a loss of material can be also hypothesized just underneath the water-sediment interface when driving velocity is high (i.e. in the free-fall coring) and the sediment is soft.

At each coring site, the equivalent layers on the adjacent FF and AD cores were correlated through peak matching on the MS logs (**Fig. 6**) defining a series of markers. MS profiles are characterized by a specific wiggle pattern resulting from a particular succession of layers with different content of magnetic minerals. Values vary between 20 and 400 x10^{-5} SI. High peak values are mostly due to high volcaniclastic content reflecting the proximity of volcanic centres that have been active with remarkable continuity in the geological time span represented by the cores.

In **figure 7** the depth from the core top of correlated magnetic susceptibility markers recognized in the AD core are plotted versus those recognized in the FF core. The figure indicates that, despite cores recovered with the FF method are longer and investigate a longer stratigraphic section than those recovered with the AD method, thickness of the same stratigraphic interval is greatly reduced. Apart from an initial lack of sediment in the FF core, the relative shortening (between the two cores) per unit length of the core (slope of the curve) varies slightly with depth. As it was expected, shortening is higher in the lower part of the core, where the sediment opposes larger resistance to corer penetration. The shallower MS marker of the AD cores is shifted by the same amount (~0.30 m) for all corings with respect to that of the FF core.

Based on the fact that at least the upper part of the cored sequences seems to be missing in the FF cores and potential shortening issues in these cores, the 'true' depths below seafloor used in the geotechnical testing are referred to the AD depths.

4.3 Geotechnical tests

Geotechnical tests were conducted on twin core samples from site A because samples of this site are finer than those at site B. Specimens selected for geotechnical testing were located within layers with the highest pelitic fraction, which ensure a better preservation of sample integrity and allows for the application of the consolidation methods for revealing soil disturbance. These layers were identified from MS trends and X-ray scans, later confirmed by laboratory grains size determination. Atterberg limits were always performed on the specimens subjected to mechanical tests. Conversely grain size, which requires a larger amount of material, at times included also the surrounding material.

The sub-bottom profiler record demonstrates unequivocally that the cores have been taken on seafloor-parallel reflectors with no indication of erosional events that may have exhumed sediment originally buried at a greater depth. In addition, the sedimentation rate calculated in the area (Sammartini et al., 2018) is between 2.24 and 2.54 mm/year between two tephra layers deposited in the last glacial, while it is reduced to an average of 0.65 mm/year during the Holocene. Thus sedimentation seems to have been continuous through time and the sediments are expected to be normally consolidated. Nevertheless, as it will be discussed in section 4.4, overconsolidation pressure, p'_c, determined from oedometer compression tests yields significant overconsolidation, especially for the shallowest samples (Table 3). Overconsolidation could result from early diagenesis or bioturbation (the latter observed in the studied cores). Similarly, values of preconsolidation pressure of 80 kPa versus an in situ effective vertical stress of 8 kPa are reported by Perret et al. (1995) for good-quality samples of clayey sediments from Canadian Fjords.

The cored sediment from which specimens for geotechnical testing were taken is a pelite made of clayey silt with a sandy fraction less than 10%. The succession contains thin beds of sandy silt or silty sand with clay fraction less than 10%. The clay-to-silt ratio increases slightly from bottom to top. The pelite has medium plasticity and remarkable homogeneity of Atterberg limits (**Tab. 3**). Grain density, ρ_s, varies within a narrow range (2.68–2.71 Mg/m^3). The sandy beds are denoted in **table 3** with an asterisk.

4.4 Oedometer tests on specimens from site A

Incremental loading oedometer compression (ILOC) tests were performed on four pairs of twin specimens. Their location in the core is reported in **figure 5**, whilst values of the initial void ratio e_0 are reported in **table 3**. Applied vertical stresses ranged between 12.5 kPa and 1.6 MPa with a standard stress ratio between successive loading steps equal to 2; each loading step lasted 24 hours. A lower initial stress would have allowed easier definition of e at the in situ stress σ'_{v0} for shallower samples. The standard value of stress ratio was chosen because of low sensitivity and silty-sandy fraction of the sediment. However, due to the overconsolidation revealed by all samples determination of pre-consolidation pressure was not affected by the two choices regarding load application.

In **figure 8** void ratio and constraint modulus M are plotted versus effective vertical stress σ'_v for the twin specimens subjected to ILOC tests. Even though M–log σ'_v plots are usually more effective for CRS tests, those reported in **figure 8** for ILOC tests highlight differences between the two sampling methods better than the e–log σ'_v curves and allow some interesting considerations. With the exception of the twin sample (AD-3-ILOC/FF-3-ILOC), in all AD samples the M–log σ'_v curve shows a sharp maximum before the yielding stress of the specimen, whilst the specimen from the FF samples virtually do not show any peak. Correspondingly, according to the M-ratio, the quality of AD1, AD2 and AD4 specimens varies from fair to very good, whilst the quality of FF specimens varies from poor to very poor. In this respect the M-ratio is less conservative than $\Delta e/e_0$ (**Tab. 3**).

The exception found for the AD3-FF3 pair could be explained by observing the different grain size of the two specimens and the anomalous values of the water content, which only in this core stretch are inverted (i.e. the water content of the FF3 specimen is higher than that of the AD3 specimen). This is likely due to an error in locating the specimens within the core.

The results of two CRS oedometer tests on twin specimens are reported in **figure 9**. As expected, the constrained modulus can be unambiguously determined but the indicators of disturbance are contradictory. In fact, in terms of constrained modulus the FF specimen shows a reduced disturbance (top of class 2) with respect to the AD specimen. Conversely, in AD specimens, $\Delta e/e_0$ is much lower and the void ratio is much higher than in FF specimens. It is worth noting that, as expected, the two compression curves join at high value of vertical stress when the structure is largely modified with respect to the original one.

In all oedometer tests, except for the AD3-FF3 pair whose scarce representativeness for disturbance evaluation has been discussed, preconsolidation pressure is higher for AD specimens. Lunne et al. (2008) found similar results on Norwegian soft clays specimens from block samples and samples taken with the NGI 54 mm sampler.

4.5 Cyclic shear tests

Three pairs of twin specimens (AD T1/FF T1, AD T2/FF T2, AD T3/FF T3) were sheared in a DSDSS device under cyclic loading. The depth with respect to the core top of the specimens is reported in **figure 5**. Physical properties and testing conditions of the six specimens subjected to the DSDSS tests are reported in **tables 3 and 4**.

Twin specimens of the same pair were loaded at the same value of σ'_v according to the "true depth" within a range of cyclic shear strain amplitudes γ_c varying between 0.0004% and 7%.

4.5.1 Shear modulus and damping ratio at very low strain

During a single loading-unloading-reloading process, the mechanical behavior of soils can be well represented by two parameters (**Fig. 4**):

- shear modulus *G;*
- damping ratio *D.*

G and D vary with the cyclic shear strain γ_c due to the non-linear behavior of soils. At large strains, i.e. above the value of γ_c at which volumetric strains appear, also the number of shearing cycles affects the two parameters.

The maximum value of the shear modulus, G_0, is measured at very low strain (in the γ_c range 0.0001% - 0.001%) where the soil behavior is assumed to be pseudo-linear.

G_0, as expected, increases with depth, i.e. moving from T1 to T3 pair (**Fig. 10** and **Tab. 5**), according to the increase in confining pressure (σ'_v). What is most interesting is that G_0 values measured on AD specimens are always higher than those measured on the twin FF specimens despite the void ratio of FF specimens is lower than that of the twin AD specimens. This result points to better preservation of soil structure in specimens collected by the AD driving technique, with respect to those collected with the FF mode. The sampling technique has also a stronger influence on G_0 than the initial void ratio does.

It is worth recalling that the lower values of e_0 in FF specimens result from a larger compression induced by the corer during the recovery of the sample. In this respect the difference in initial void ratio between the twin specimens is smaller at higher sampling depth, where the corer applies a smaller force to the sediment.

Values of small-strain damping D_0 provided by DSDSS tests fall within the typical range for fine-grained soils excepting the value for the FF T1 specimen, lower than the other ones. Unfortunately, no identification test could be done on this specimen to relate D_0 to the intrinsic properties of the sediment. However test interpretation has to take into account that accuracy of D_0 values is lower than those of G_0 due to the effect of electrical noise on the shape of the stress-strain loops (see definition of D in **figure 4**)

4.5.2 Variation of shear modulus and damping ratio with strain amplitude

The values of the equivalent shear modulus determined for the different steps at increasing shear strain amplitude were normalized with respect to G_0 to obtain the G/G_0 - γ_c curve showed in **figure 11**.

The G_{eq}/G_0 - γ_c curves do not provide clear indications on the influence of the two different sampling methods on the variation of the dynamic stiffness with magnitude of cyclic strain.

This result can be explained by considering that once γ_c exceeds the threshold marking the stress-strain linear behaviour (i.e. the sub-horizontal stretch of the curve) the original soil structure is largely lost and the curve shape depends on parameters other than structure (e.g. plasticity, grain size).

The D - γ_c curves plotted in **figure 12** show that over most of the γ_c range AD specimens of the T1 and T3 pairs exhibit a less dissipative behaviour than the corresponding FF specimens, whilst curves of the T2 pair lie close to each other.

5. Discussion of results

Magnetic susceptibility measurements and laboratory geotechnical investigations conducted on twin cores recovered with two different coring devices provided indications of disturbance produced by the two sampling methods. In particular we evaluate disturbance reduction offered by the controlled penetration speed Angel Descent technique (AD) with respect to the conventional free-fall (FF) procedure. Other disturbance factors, as that due to specimen preparation should have been not significant by considering the experience in geotechnical testing and handling of marine sediment samples of all operators involved in testing activities (CNR, OGS, DISG-Sapienza and DGM-CSIC).

Magnetic signature of the susceptibility logs, in the form of either single peaks or peak sequences, proved to be an effective tool in detecting differences in apparent depth (i.e. from the core top) of the same horizons in twin cores and hence to better evaluate core shortening. This procedure requires that horizons with magnetic susceptibility sharply higher than that of the sandwiching sediments must be frequent in the cored succession. In the studied area, as in many other regions worldwide, this task is favoured by the proximity to onshore volcanoes that have spread several tephra layers over a wide area over a long time span. Improvements in log comparison could be made by using mathematical correlations techniques, which are beyond the scope of this article. No core logging data are available in addition to MS, nor can we support the observed shortening with anomalies in density or water content. In our opinion, given the high resolution sapling of the MS values and the high MS contrasts within the sediments, this parameter is sufficient for core-to core-correlation between twin cores and therefore to calculate accurately the relative shortening.

In spite of a significant shortening, sharp bending of laminae near the core walls has been never seen on X-ray scans. In our opinion, this can be explained with an overall volume reduction of the sediment, which takes place due to a relatively fast dissipation of excess pore pressure induced by sampling, favoured by the silty-sandy layers, coupled to an overall significant stiffness of the sediment.

Different aspects of the geotechnical behavior of the sediment were utilized to provide a mechanically-based quantitative estimate of sediment disturbance: i) the well-known disturbance index based on the void ratio in the initial state and at recompression under the in situ vertical stress; ii) the shape of compressibility curves; iii) the shape of plots of constrained moduli versus vertical effective stress (and associated "modulus ratio"); iv) cyclic properties.

Values of $\Delta e/e_0$ of AD specimens were always lower than those of FF specimens and in a couple of specimens they even reached the "good quality" threshold. Curves at points ii) did not provide coherent results. More encouraging is the shape of plots of M versus void ratio or vertical strain. In this respect the presence of a non-negligible silty-sandy fraction especially in form of thin laminae, different for a pair of twin specimens, could have slightly differentiated the behavior of twin specimens. A prevailing silt content and a slight sandy fraction can "round" curvature change of compressibility and M - e curves from oedometer tests and increase drainage during sampling, thus allowing volume changes. In this respect it is worth recalling limitations to the applicability of these procedures in soils which do not have a prevailing clay fraction, expressed by Krage et al. (2015). Furthermore is to be noted that Lunne et al. (2006) recommend to use the criterion based on $\Delta e/e_0$ for marine clays having an OCR not higher than 4.

An unambiguous answer was instead given by cyclic shear tests, especially in the form of low-strain stiffness G_0. This parameter, very sensitive to the soil structure, can highlight small changes induced by sampling operations. Differences in G_0 were also detected by Tan et al. (2002) between soft-clay specimens from samples recovered with conventional and Japanese thin-walled tube samplers. Conversely the cyclic behavior at higher strains, relates more to testing-induced soil structural changes than to the initial quality of the samples.

6. Conclusions

The use of a gravity piston corer equipped with a device controlling corer speed at the impact and during penetration demonstrated to significantly reduce core disturbance with respect to the conventional free-fall technique. Reduction of disturbance was mostly highlighted by the analysis of the core shortening through the comparison of magnetic susceptibility logs and the comparison of low strain shear stiffness, determined by means of cyclic simple shear tests. In this respect, if magnetic horizons were rarer than at the studied site, logs of other properties could be utilized as shown, among others, by Govin et al. (2016), who also point out the need of reducing coring speed.

This study provides an additional evidence of the possibility of significantly reducing core disturbance using small-diameter cylindrical sampling devices deployed by research vessels that may avoid the use of expensive large-diameter block-samples deployed by drilling vessels, platforms or barges.

Evidence was obtained on sediments having a high silty fraction and a significant coarse-grained fraction, which, despite their large diffusion in the marine environment, have been object of disturbance assessment studies only in relatively recent times. However, authors hope they can extend this study to sediments characterized by higher clay content and rarer coarse-grained horizons, which should ensure application of disturbance assessment from oedometer compression test results, and higher penetration, respectively.

7. Acknowledgments

DSDSS device was kindly made available by Prof. G. Lanzo at Department of Structural and Geotechnical Engineering of Sapienza University of Rome. Cyclic and part of identification tests were performed by Mr. S. Silvani and Mr. Maurizio Di Biase of DISG and Anita Di Giulio of CNR-IGAG, who are warmly acknowledged. Thanks are due to Antonio Mercadante (formerly at IAMC-CNR) acknowledged for on board magnetic susceptibility measurements. Authors acknowledge MARUM, University of Bremen, for digital X-ray scans of AD and FF cores. R. Urgeles and J. Llopart acknowledge funding from project INSIGHT (CTM2015-70155-R) jointly funded by the Spanish *Ministerio de Economía y Competitividad* and the European Regional Development Fund. The research was funded by grants awarded to FB, AC and PT from the *National Research Program Flagship Projects RITMARE* – The Italian Research for the Sea - coordinated by the Italian National Research Council. Finally Authors thanks one of the reviewers for the useful comments and suggestions that improved the manuscript.

8. References

Andresen, A., Kolstad, P., 1979. *The NGI 54 sampler for undisturbed sampling of clays and representative sampling of coarser materials*. In: Proceedings of the International Symposium on Soil Sampling, Singapore, I.S.S.M.F.E., pp. 13–21.

Andresen, A., 1981. *Exploration, sampling and in-situ testing of soft clay*. In Soft clay Engineering. Brand, E.W., Brenner, R.P. (Eds.), Developments in Geotechnical Engineering, vol. 20. Elsevier, pp. 245–308.

Bellonia, A., Budillon, F., Trincardi, F., Insinga, D., Iorio, M., Asioli, A., Marsella, E., 2008. *Licosa and Acciaroli submarine slides, Eastern Tyrrhenian margin: characterisation of a possible common weak layer*. Rendiconti online Soc. Geol. It., 3:83-84.

Bourillet, J-F., Damy, G., Dussud, L., Sultan, N., Woerther, P., Migeon S., 2007. *Behaviour of a piston corer from accelerometers and new insights on quality of the recovery*. Proceedings of the 6th International Off shore Site Investigation and Geotechnics Conference: Confronting New Challenges and Sharing Knowledge, London, 127-132.

Chaney, R.C., Almagor, G., 2015. Seafloor Processes and Geotechnology. CRC Press, Boca Raton, 558 pp, ISBN 9781482207408.

D'Elia, B., Lanzo, G., Pagliaroli, A., 2003. *Small-strain stiffness and damping of soils in a direct simple shear device*. 7th Pacific Conference on Earthquake Engineering, Christchurch, New Zealand, CD Rom, Paper No. 111, 8 pp.

Donohue, S., Long, M., 2010. *Assessment of sample quality in soft clay using shear wave velocity and suction measurements*. Géotechnique 60, 11: 883-889. doi:10.1680/geot.8.T.007.3741.

Douroudian, M., Vucetic, M., 1995. *A Direct Simple Shear Device for Measuring Small-Strain Behavior.* Geotechnical Testing Journal, 1995, 18 (1): 69-85.

Dück, Y., Liu, L., Lorke, A., Ostrovsky, I., Katsman, R., Jokiel, C., 2019. *A novel freeze corer for characterization of methane bubbles and assessment of coring disturbances*. Limnology and Oceanography: Methods, 17(5):1-15.

Emery K.O., Dietz, R.S., 1941. *Gravity coring instrument and mechanics of sediment coring*. Bulletin of the Geological Society of America, 52:1685-1714.

Gallmetzer, I., Haselmair, A., Stachowitsch, M., Zuschin, M., 2016. *An innovative piston corer for large-volume sediment samples*. Limnology and Oceanography: Methods,14, 698-717.

Garziglia, S., 2010. Typologie, phénoménologie et approche des facteurs déclenchants des glissements sous-marins: application aux deltas profonds du Nil et du Niger Thèse de doctorat). Université de Nice-Sophia Antipolis. Faculté des sciences, France, 370 pp.

Govin, A., Vázquez Riveiros, N., Réaud, Y., Waelbroeck, C. and Giraudeau, J., 2016. *Unprecedented coring performance with the upgraded Research Vessel Marion Dufresne*. PAGES Magazine, 24(1):27.

Heffler, D., 1991. *Piston Corer Dynamics*, Proceedings ofOceans91: Ocean Technologies and Opportunities in the Pacific for the 90's, 3:1587-1591, IEEE, Piscataway, NJ.

Hight, D.W., Leroueil, S., 2003. *Characterization of soils for engineering purposes*. Proc. Int. Workshop on Characterization and Engineering Properties of Natural Soils, Singapore, 1: 255-360.

Karlsrud K., Hernandez-Martinez, F.G., 2013. *Strength and deformation properties of Norwegian clays from laboratory tests on high-quality block samples*. Can. Geotech. J. 50(12), 1273-1293.

Krage, C.P., DeJong, J.T., De Groot, D.J., Dyer, A.M., Lukas, W.G., 2015. *Applicability of Clay-Based Sample Disturbance Criteria to Intermediate Soils*, 6th International Conference on Earthquake Geotechnical Christchurch, New Zealand

Heffler, D., 1991. *Piston corer dynamics*. Proc. Int. Conf. OCEANS '91. 'Ocean Technologies and Opportunities in the Pacific for the 90's'.1587-1591. IEEE Xplore. doi:10.1109/OCEANS.1991.606532

Iorio, M., Liddicoat, J., Budillon, F., Incoronato, A., Coe, R.S., Insinga, D.D., Cassata W.S., Lubritto, C., Angelino, A., Tamburrino, S., 2014. *Combined palaeomagnetic secular variation and petrophysical records to time-constrain geological and hazardous events: An example from the eastern Tyrrhenian Sea over the last 120 ka*. Global and Planetary Change 113, 91–109

Jeanjean, P., Hampson, K., Evans, T., Liedtke, E.,Clukey, E.C., 2005. *An operator's perspective on offshore risk assessment and geotechnical design in geohazard-prone areas*. In Frontiers in Offshore Geotechnics ISFOG 2005, S. Gourvenec& M. Cassidy Eds., 115-144. Taylor & Francis/Balkema, Leiden.

Jamiolkowski, M., Ladd, C.C., Germaine, J.T., Lancellotta, R., 1985. *New developments in field and laboratory testing of soils - Theme Lecture*. Proc. llth ICSMFE, San Francisco, 1: 57-152. Balkema.

Jutzeler, M., J. D. L. White, P. J. Talling, M. McCanta, S. Morgan, Le Friant, A., and Ishizuka, O., 2014. Coring disturbances in IODP piston cores with implications for offshore record of volcanic events and the Missoula megafloods, Geochem. Geophys. Geosyst., 15, 3572–3590, doi: 10.1002/2014GC005447.

Ladd, C.C., DeGroot, D.J., 2003. *Recommended practice for soft ground site characterization: Arthur Casagrande lecture*. Proc., 12thPanamerican Conf. on Soil Mechanics and Geotechnical Engineering, Boston, 3-57.

Landon M.M., DeGroot, D.J., Sheahan, T.C., P.E., 2007. *Nondestructive Sample Quality Assessment of a Soft Clay Using Shear Wave Velocity*. J. Geotech. Geoenviron. Eng. 133(4): 424-432. doi:10.1061/(ASCE)1090-0241(2007)133:4(424).

Lanzo, G., Pagliaroli, A., Tommasi, P., Chiocci, F. L., 2009. *Simple shear testing of sensitive, very soft offshore clay for wide strain range*. Canadian Geotechnical Journal, 46(11), 1277-1288.

Lee, J.Y., Jung, J.W., Lee, M.H., Bahk, J.-J., Choi, J., Ryu, B.-J., and Schultheiss P., 2013. *Pressure core based study of gas hydrates in the Ulleung Basin and implication for geomechanical controls on gas hydrate occurrence*. Marine and Petroleum Geology 47:85-98.

Lunne, T., Berre, T., Strandvik, S., 1997. *Sample disturbance effects in soft low plastic Norwegian clay*. In Proceedings of the Conference on Recent Developments in Soil and Pavement Mechanics, Rio de Janeiro, June 1997, pp. 81-102.

Lunne, T., Berre, T., Andersen K.H., Strandvik, S., Sjursen, M., 2006. *Effects of sample disturbance and consolidation procedures on measured shear strength of soft marine Norwegian clays*. Canadian Geotechnical Journal, 43, pp 726-750.

LunneT., Long, M., 2006. *Review of long seabed samplers and criteria for new sampler design*. Marine Geology 226: 145-165.

Lunne T., Berre T., Andersen, K.H., Sjursen, M., Mortensen, N., 2008. *Effects of sample disturbance and consolidation procedures on measured shear strength of soft marine Norwegian clays*. Geotechnical and Geophysical Site Characterization – Huang & Mayne (eds), Taylor & Francis Group, London, ISBN 978-0-415-46936-4.

Lukas W., 2018. *An experimental investigation of the influence of sampling on the behavior of intermediate soils*. Doctoral Dissertations. 1198. https://scholarworks.umass.edu/dissertations_2/1198.

Magagnoli, M., 2017. *A new coring method in deep water*. Marine Georesources and Geotechnology, 35/4, 496-503.

Montarges R., Le Tirant P., Wannesson, J., Valery P., Berthon, J.L., 1983. *Large-size Stationary Piston Corer*, 2nd International Conference on Deep Offshore Technology, 63-74.

Perret, D., Locat, J., Leroueil, S., 1995. *Strength development with burial in fine-grained sediments from the Saguenay Fjord, Quebec*. Canadian Geotechnical Journal 32, 247–262. doi:10.1139/t95-027

Sammartini, M., Camerlenghi, A., Budillon, F., Insinga, D.D., Zgur, F., Conforti, A., Iorio, M., Romeo, R., and Tonielli, R., 2018. *Open-slope, translational submarine landslide in a tectonically active volcanic continental margin (Licosa submarine landslide, southern Tyrrhenian Sea)*. Geological Society, London, Special Publications, 477, 24 May 2018, https://doi.org/10.1144/SP477.34

Schilling, J., Van Weering, T.C.E. and Eisma, D., 1988. *Advantages of light-weight kevlar rope for ocean bottom sampling with the piston corer and box corer*. Marine Geology, 79:149-152.

Shimono, T., Yamazaki, T. and Inoue, S., 2014. *Influence of sampling on magnetic susceptibility anisotropy of soft sediments: comparison between gravity and piston cores*. Earth, Planets and Space, 66:3, 8 pp., https://doi.org/10.1186/1880-5981-66-3.

Skinner, L.C., McCave, I.N., 2003. *Analysis and modelling of gravity- and piston coring based on soil mechanics*. Marine Geology, 199:181-204.

Taleb, F., Garziglia, S. and Sultan, N., 2018. *In situ characterisation of gas hydrate-bearing clayey sediments in the Gulf of Guinea*. Cone Penetration Testing 2018, Hicks, Pisanò & Peuchen (Eds.), CRC Press, ISBN 978-1-138-58449-5599-604.

Tan, T.S., Lee, F.H., Chong, P.T., Tanaka, H., 2002. *Effect of sampling disturbance on properties of Singapore clay*.J. Geotech. Geoenviron. Eng., 128(11):898-906.

Villinger, H., Grigel, J., Heesemann, B., 1999. *Acceleration-monitored coring revisited*. Geo-Marine Letters, 19:275-281.

Figure captions

Figure 1. Location of coring sites A and B off the South Tyrrhenian coast.

Figure 2. Subbottom chirp seismic profiles at coring sites A (a), B2 (b) and B3 (c).

Figure 3. Scheme (a) and detail (b) of the DSDSS device.

Figure. 4. Definition of the equivalent shear modulus (G_{eq}) and damping ratio (D). G_0 is the maximum shear modulus, ΔW is the dissipated energy per unit volume (area within the reloading-unloading cycles), τ_c is the stress amplitude.

Figure 5. Kinematical parameters of the A-FF and A-AD cores (on the left and right, respectively). Negative velocities are downward velocities

Figure. 6. Susceptibility logs and RX digital images of the twin cores at site A, and location of the twin specimens subject to geotechnical testing (a). Susceptibility logs of the two couples of twin cores at site B with peak correlation (b).

Figure 7. Distance, D, from the core top of magnetic susceptibility markers: AD values vs. FF values.

Figure 8. Plots of void ratio e (a) and constrained modulus M (b) versus effective vertical stress for the twin specimens subjected to ILOC tests. Full dots and black lines refer to AD samples; empty circles and grey lines refer to FF samples.

Figure 9. Plots of void ratio e (upper curves) and constrained modulus M (lower curves) versus effective vertical stress σ'_v for the twin specimen subjected to CRS oedometer compression tests. For symbols, see figure 8.

Figure 10. Equivalent shear modulus G_{eq} versus cyclic shear strain amplitude γ_c.

Figure 11. Normalized equivalent shear modulus G_{eq}/G_0 versus cyclic shear strain amplitude γ_c.

Figure 12. Variation of damping ratio D at low strains versus cyclic shear strain amplitude γ_c.

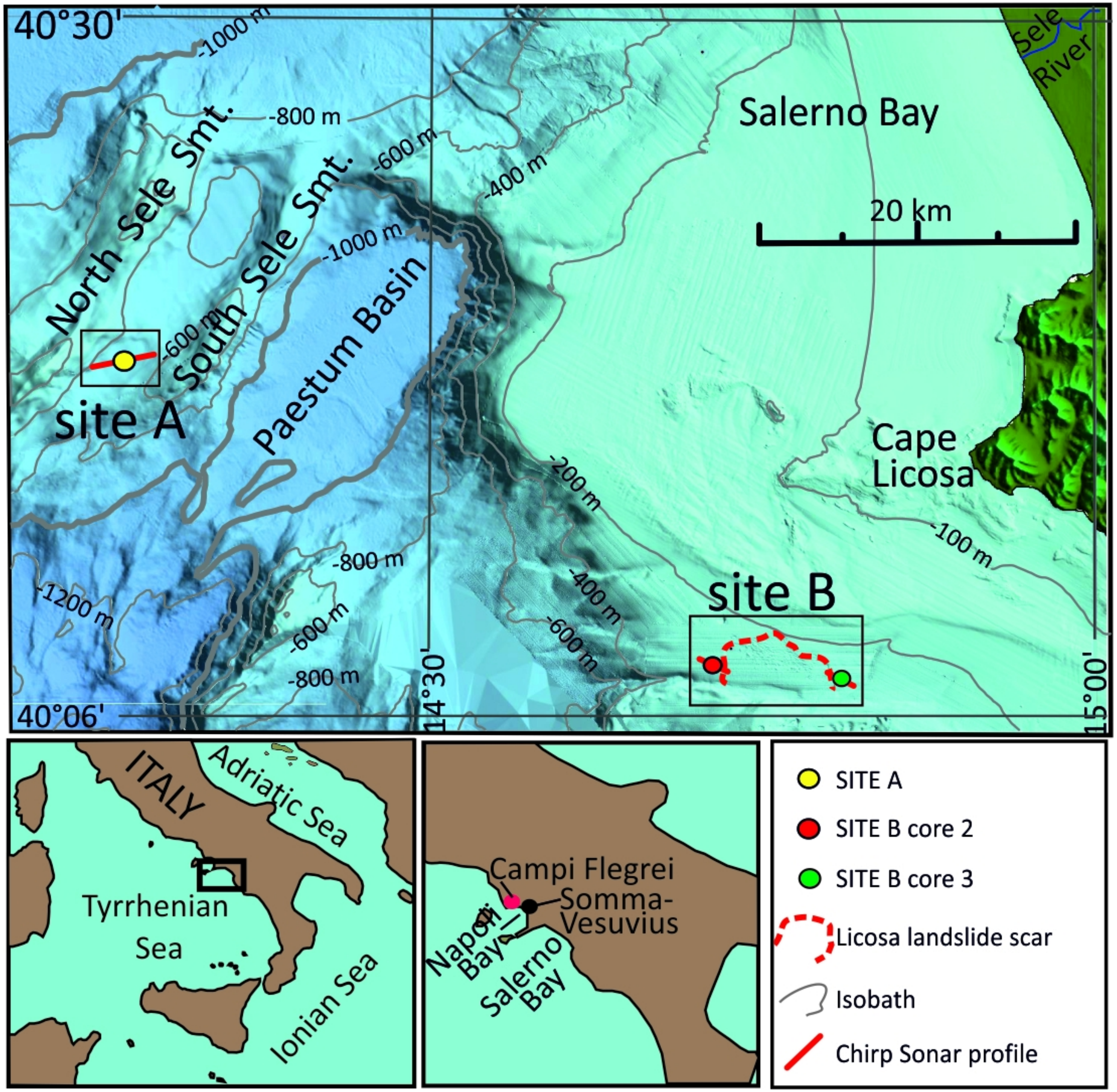

40°30'
40°06'
14°30'
15°00'
-1000 m
-800 m
-600 m
-400 m
-200 m
-100 m
-1200 m
North Sele Smt.
South Sele Smt.
Paestum Basin
Salerno Bay
Sele River
20 km
Cape Licosa
site A
site B
ITALY
Adriatic Sea
Tyrrhenian Sea
Ionian Sea
Campi Flegrei
Somma-Vesuvius
Napoli Bay
Salerno Bay
SITE A
SITE B core 2
SITE B core 3
Licosa landslide scar
Isobath
Chirp Sonar profile

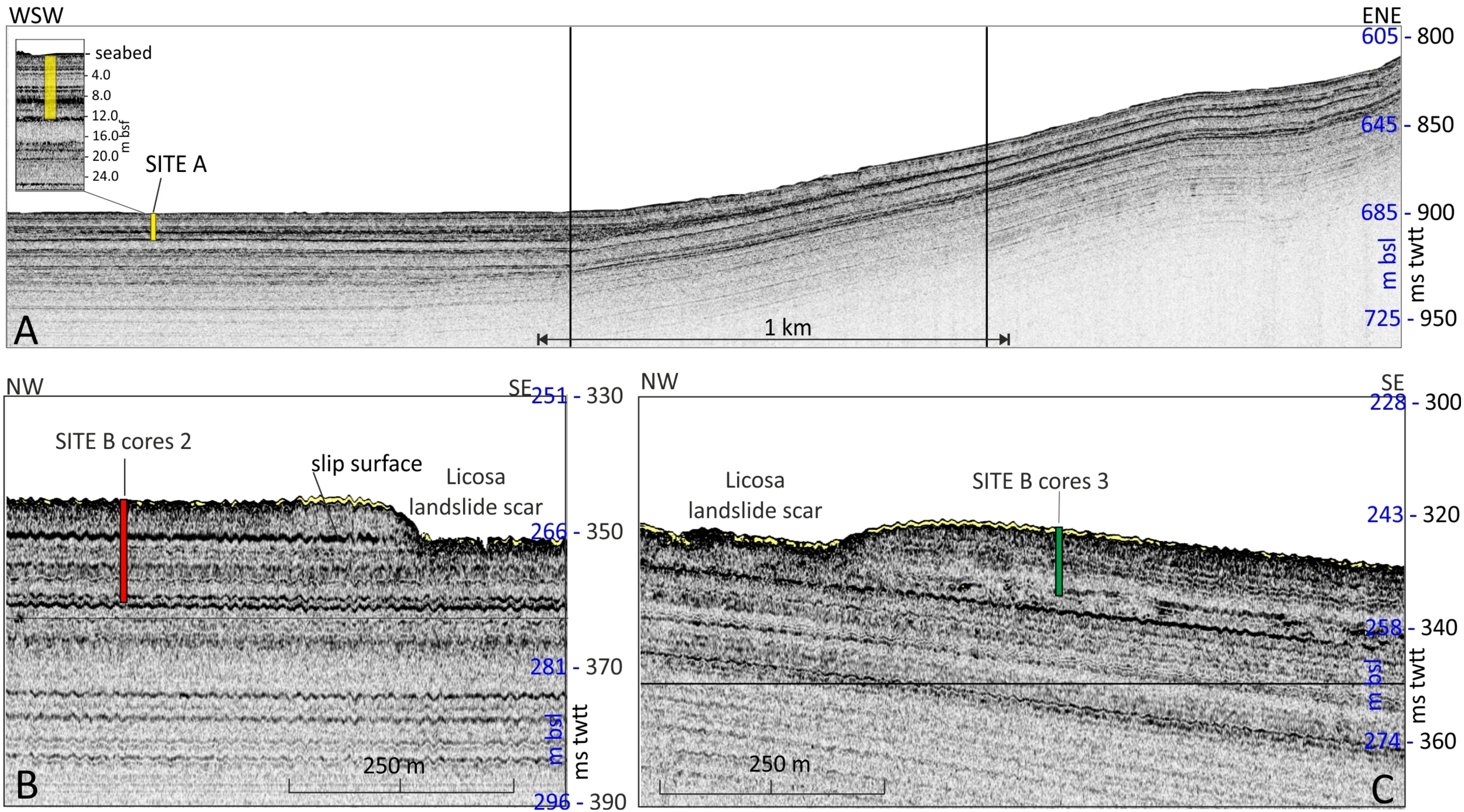

WSW
ENE
seabed
4.0
8.0
12.0
16.0
20.0
24.0
m bsf
SITE A
605 - 800
645 - 850
685 - 900
725 - 950
m bsl
ms twtt
1 km
A
NW
SE
251 - 330
266 - 350
281 - 370
296 - 390
SITE B cores 2
slip surface
Licosa landslide scar
250 m
B
NW
SE
228 - 300
243 - 320
258 - 340
274 - 360
Licosa landslide scar
SITE B cores 3
250 m
C

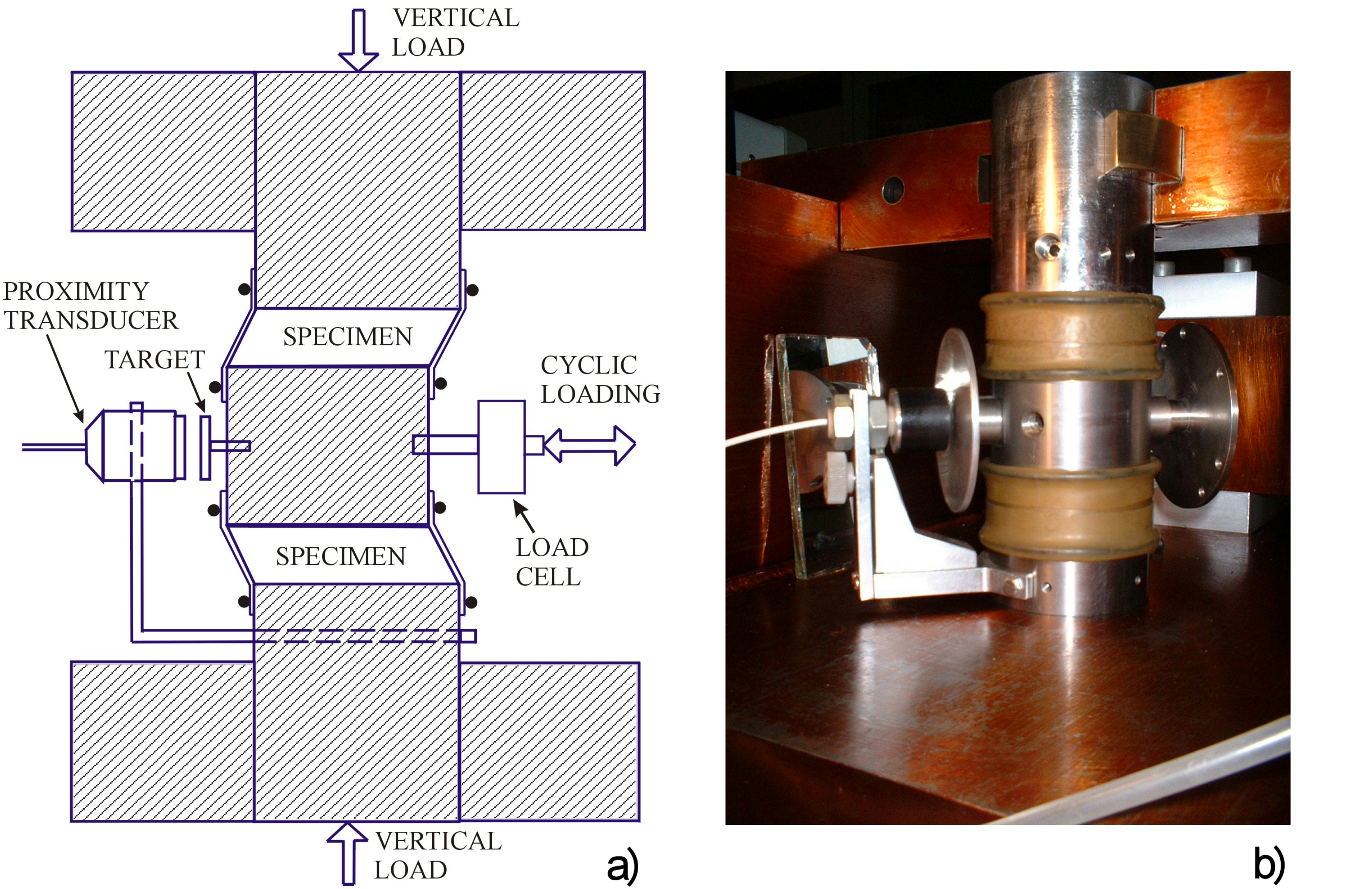
VERTICAL LOAD
PROXIMITY TRANSDUCER
TARGET
SPECIMEN
CYCLIC LOADING
SPECIMEN
LOAD CELL
VERTICAL LOAD
a)
b)

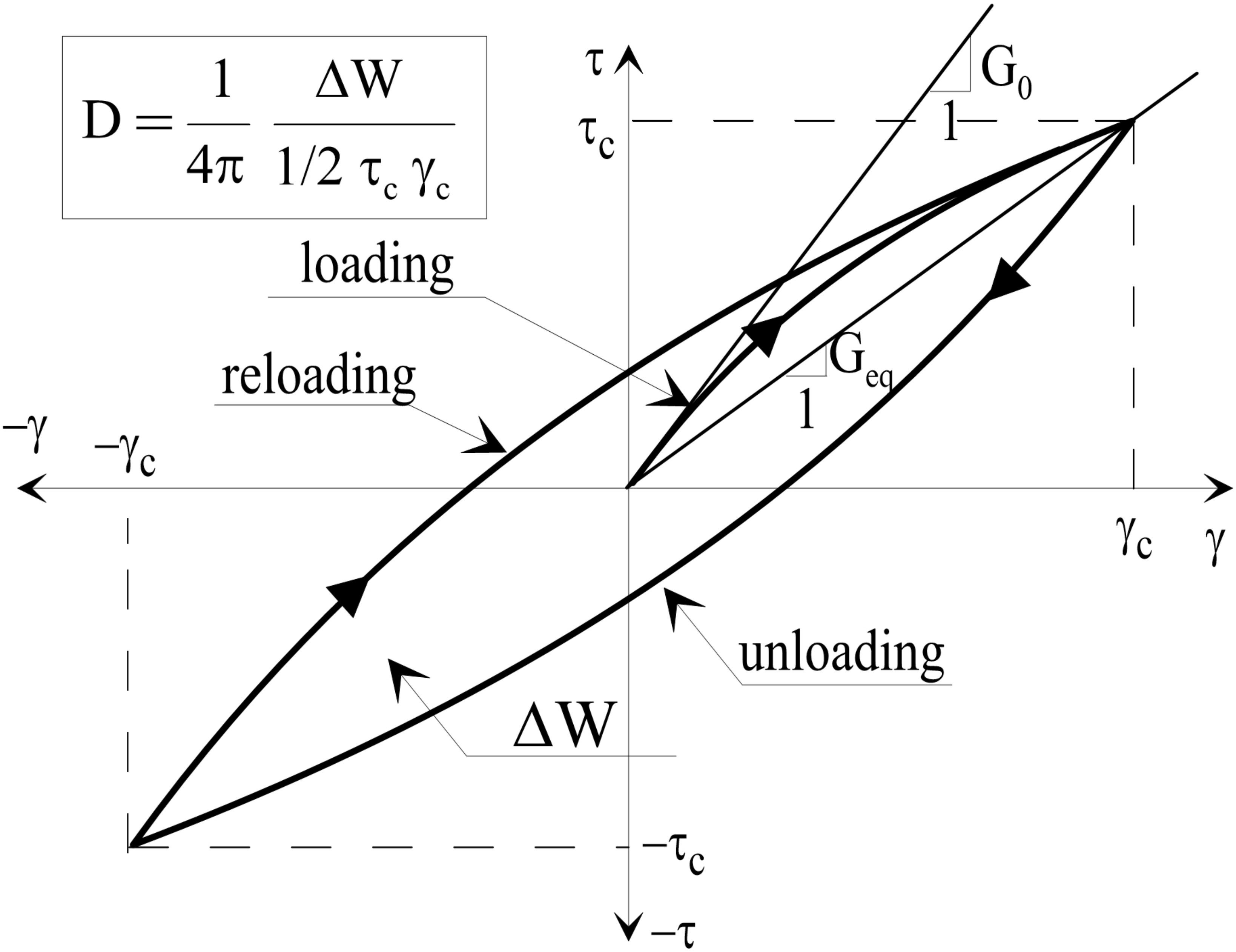

$D = \frac{1}{4\pi} \frac{\Delta W}{1/2\ \tau_c\ \gamma_c}$
τ
τ_c
G_0
1
loading
reloading
G_{eq}
1
$-\gamma$
$-\gamma_c$
γ_c
γ
unloading
ΔW
$-\tau_c$
$-\tau$

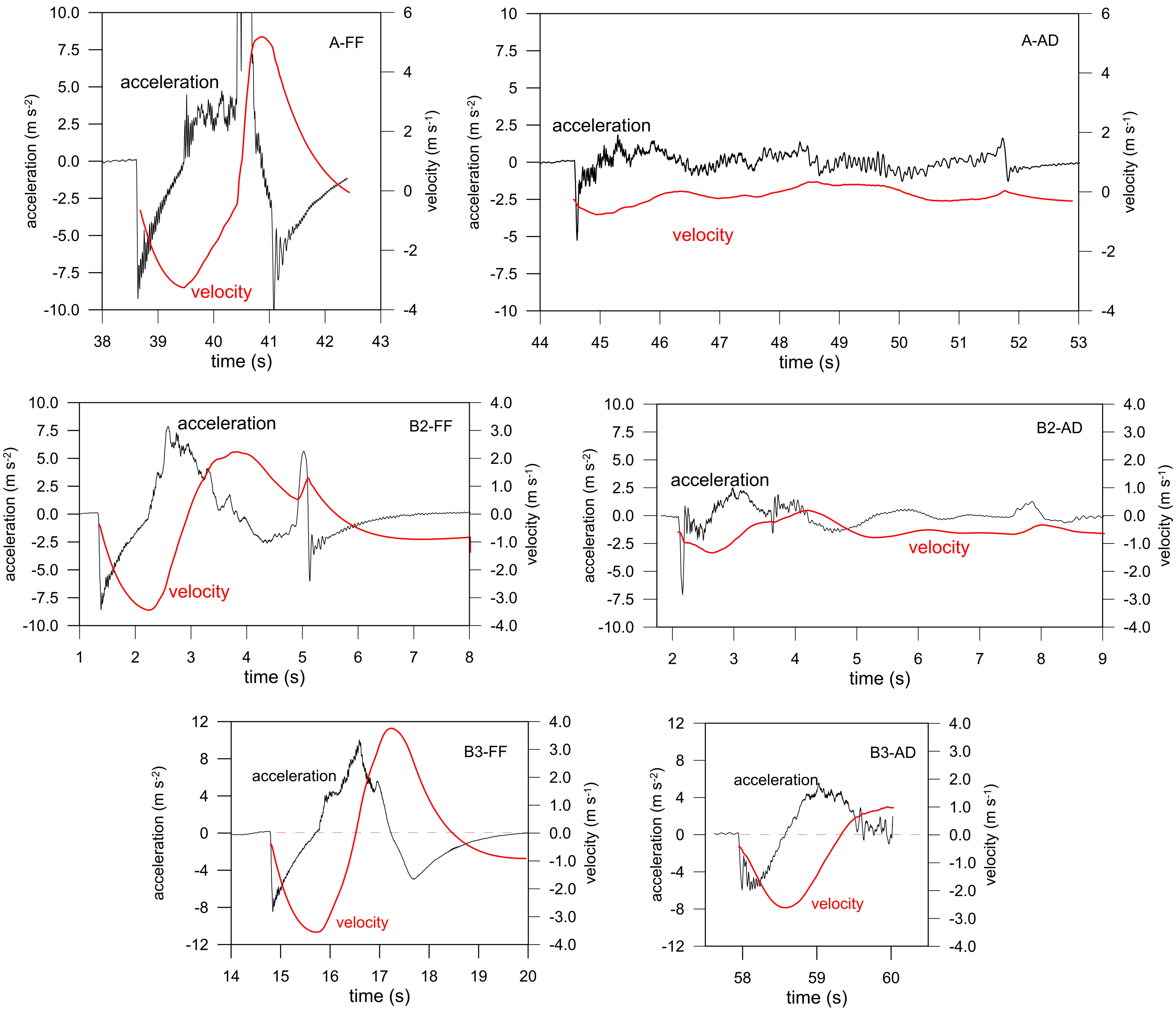
A-FF
acceleration
velocity
acceleration (m s-2)
velocity (m s-1)
time (s)
A-AD
acceleration
velocity
acceleration (m s-2)
velocity (m s-1)
time (s)
B2-FF
acceleration
velocity
acceleration (m s-2)
velocity (m s-1)
time (s)
B2-AD
acceleration
velocity
acceleration (m s-2)
velocity (m s-1)
time (s)
B3-FF
acceleration
velocity
acceleration (m s-2)
velocity (m s-1)
time (s)
B3-AD
acceleration
velocity
acceleration (m s-2)
velocity (m s-1)
time (s)

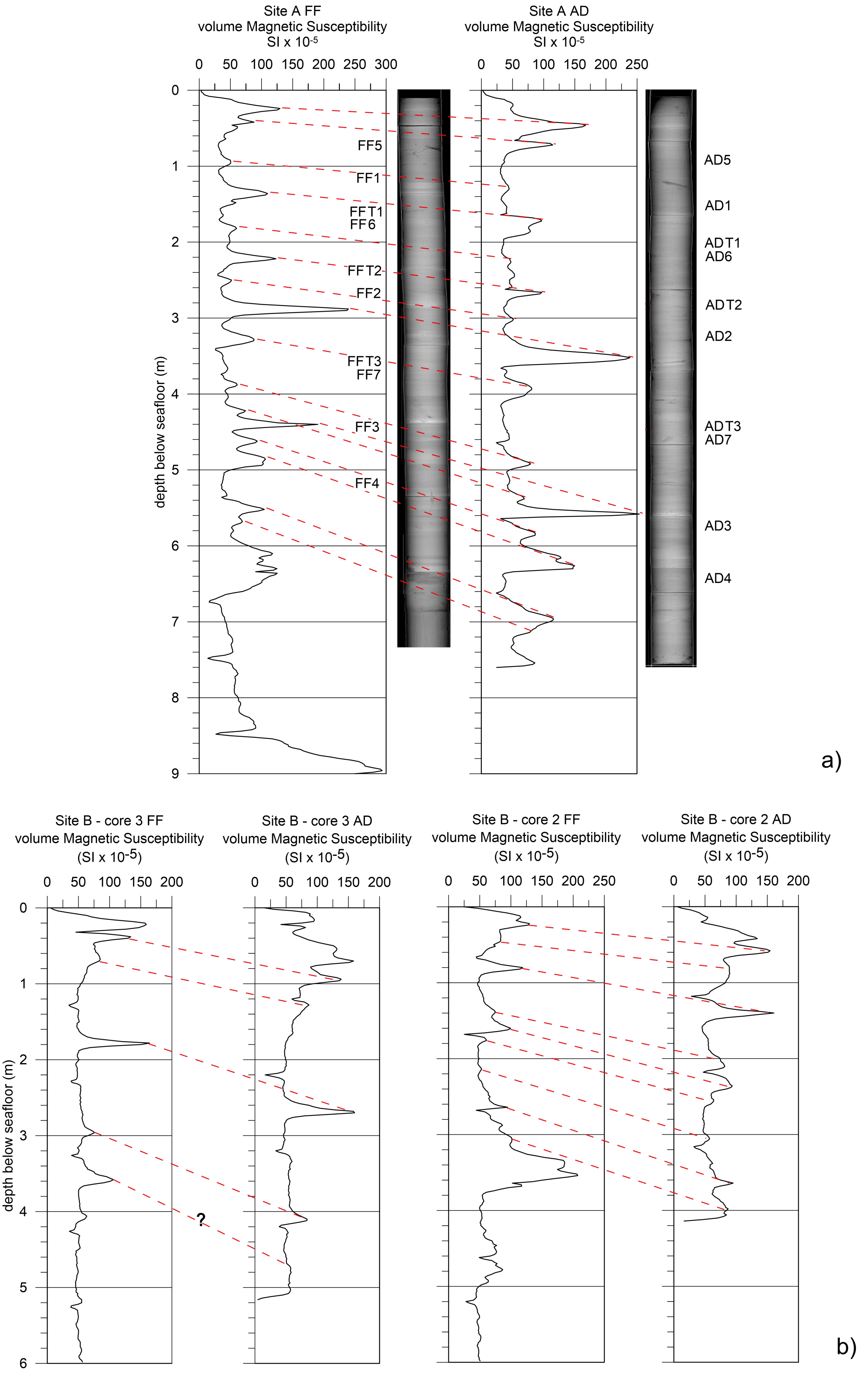
Site A FF
volume Magnetic Susceptibility
SI x 10-5
0 50 100 150 200 250 300
Site A AD
volume Magnetic Susceptibility
SI x 10-5
0 50 100 150 200 250
depth below seafloor (m)
0 1 2 3 4 5 6 7 8 9
FF5
FF1
FFT1
FF6
FFT2
FF2
FFT3
FF7
FF3
FF4
AD5
AD1
ADT1
AD6
ADT2
AD2
ADT3
AD7
AD3
AD4
a)
Site B - core 3 FF
volume Magnetic Susceptibility
(SI x 10-5)
0 50 100 150 200
Site B - core 3 AD
volume Magnetic Susceptibility
(SI x 10-5)
0 50 100 150 200
Site B - core 2 FF
volume Magnetic Susceptibility
(SI x 10-5)
0 50 100 150 200 250
Site B - core 2 AD
volume Magnetic Susceptibility
(SI x 10-5)
0 50 100 150 200
depth below seafloor (m)
0 1 2 3 4 5 6
?
b)

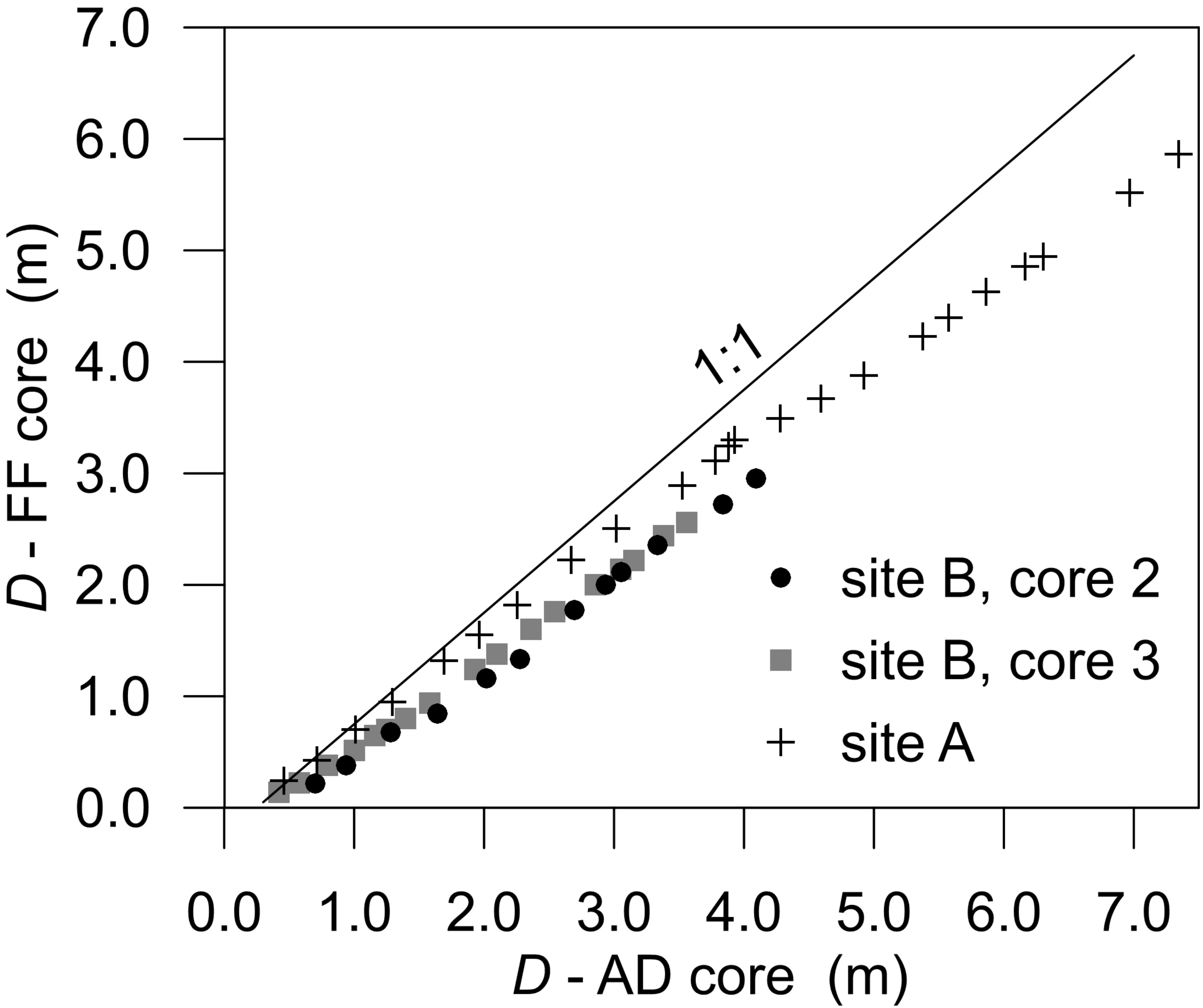

7.0
6.0
5.0
4.0
3.0
2.0
1.0
0.0
D - FF core (m)
1:1
site B, core 2
site B, core 3
site A
0.0
1.0
2.0
3.0
4.0
5.0
6.0
7.0
D - AD core (m)

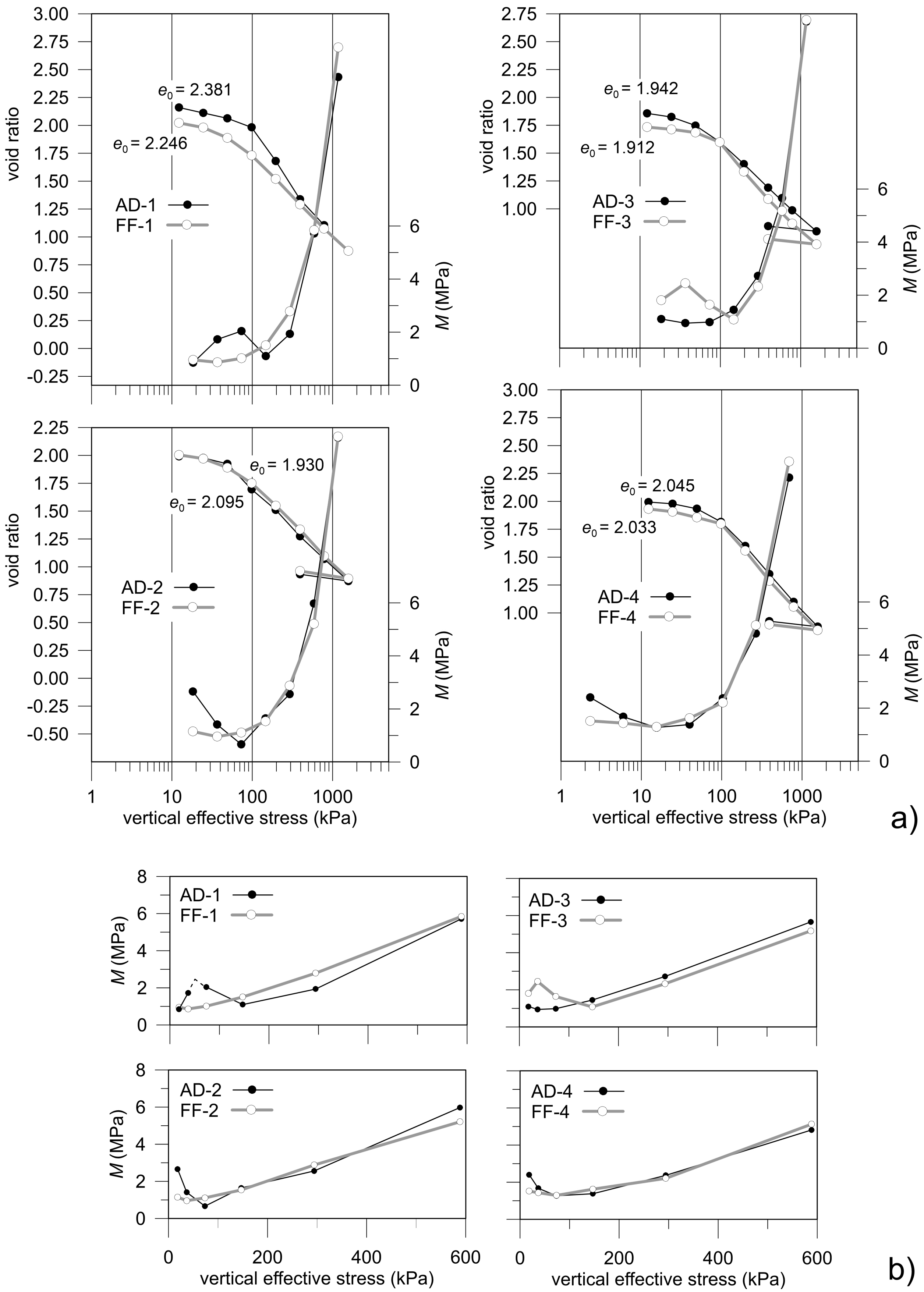

void ratio
e_0 = 2.381
e_0 = 2.246
AD-1
FF-1
M (MPa)
e_0 = 1.942
e_0 = 1.912
AD-3
FF-3
e_0 = 1.930
e_0 = 2.095
AD-2
FF-2
e_0 = 2.045
e_0 = 2.033
AD-4
FF-4
vertical effective stress (kPa)
a)
b)

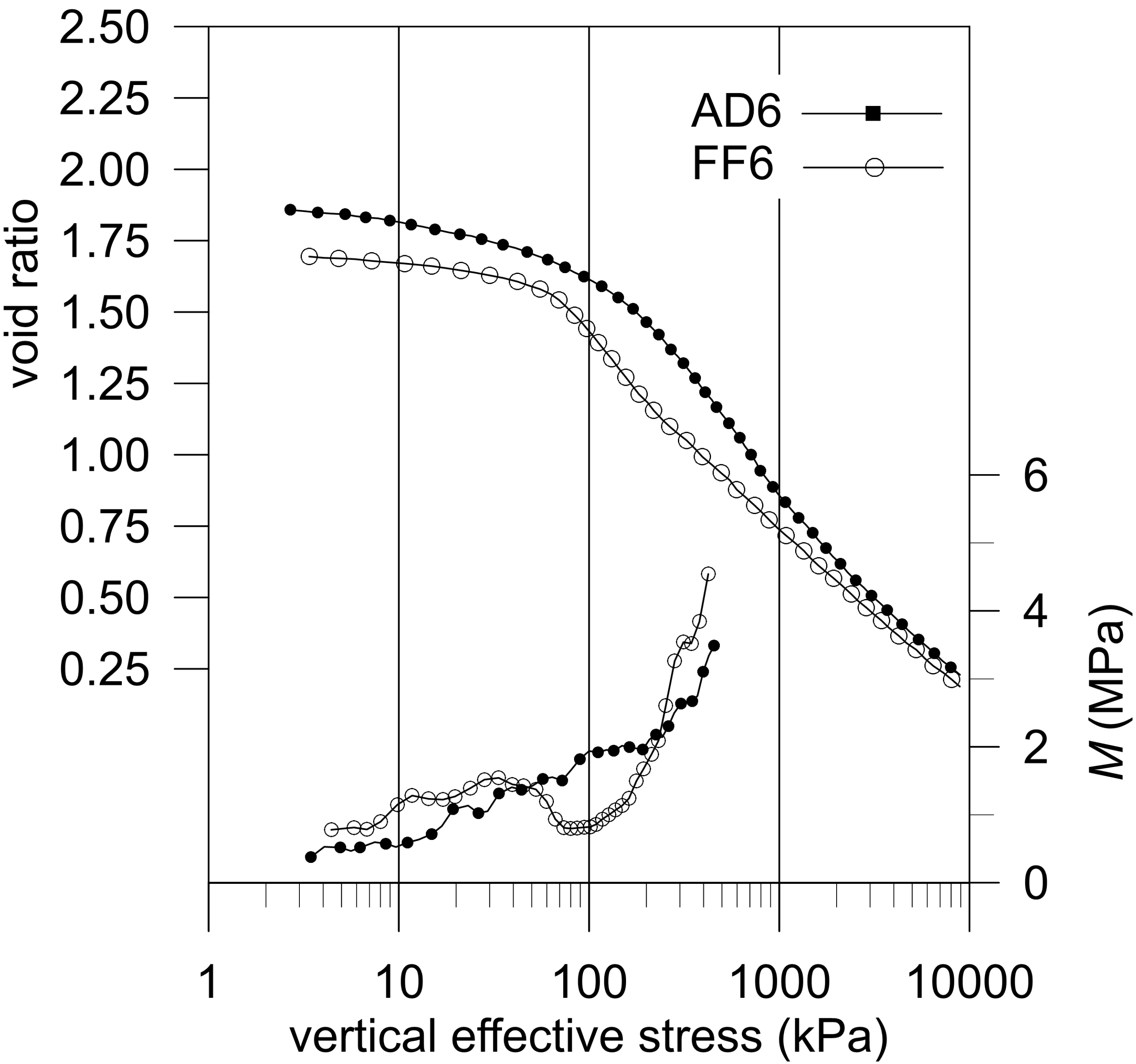

2.50
2.25
2.00
1.75
1.50
1.25
1.00
0.75
0.50
0.25
void ratio
AD6
FF6
6
4
2
0
M (MPa)
1
10
100
1000
10000
vertical effective stress (kPa)

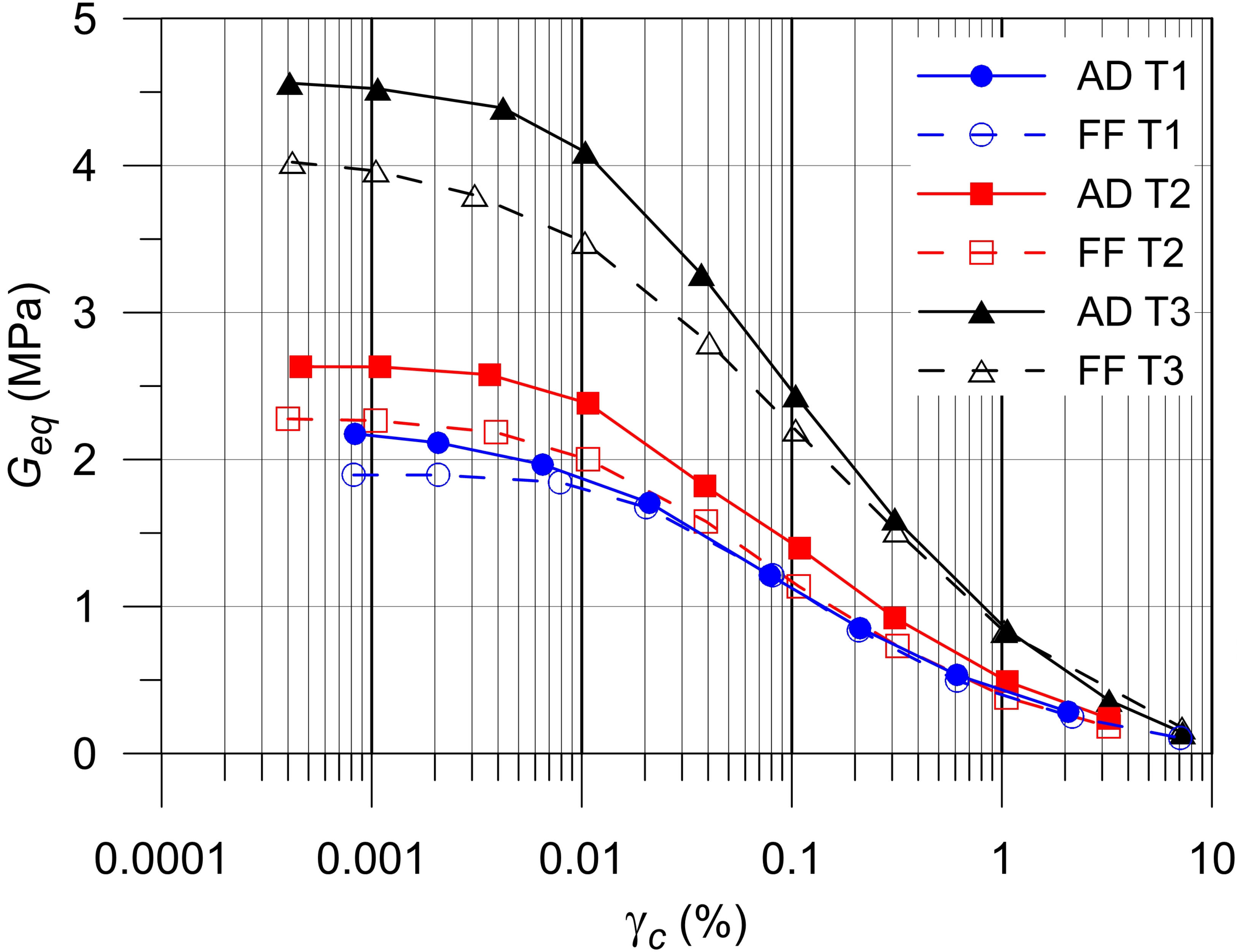

5
4
3
2
1
0
G_{eq} (MPa)
0.0001
0.001
0.01
0.1
1
10
γ_c (%)
AD T1
FF T1
AD T2
FF T2
AD T3
FF T3

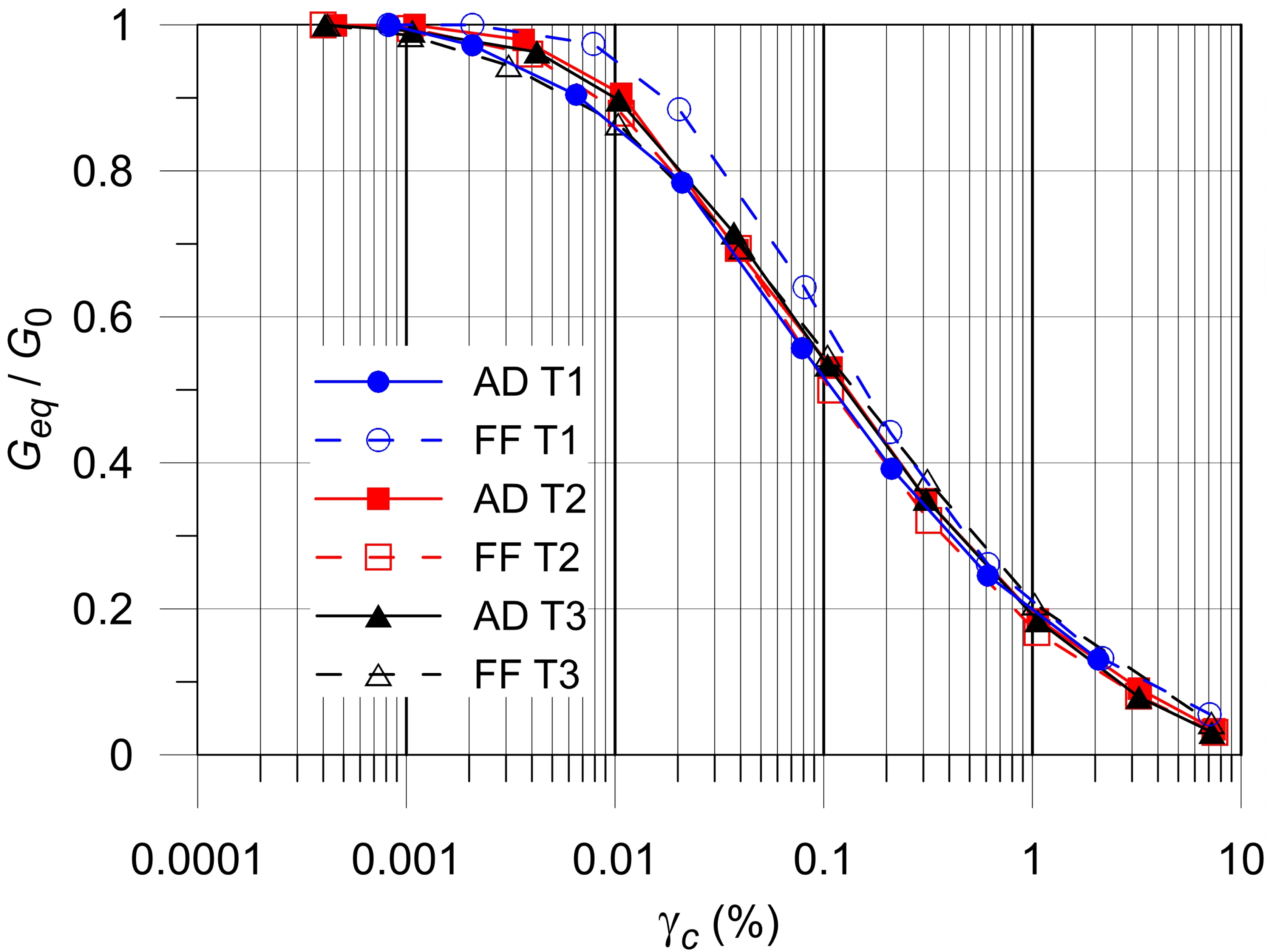

1
0.8
0.6
0.4
0.2
0
G_{eq} / G_0
0.0001
0.001
0.01
0.1
1
10
γ_c (%)
AD T1
FF T1
AD T2
FF T2
AD T3
FF T3

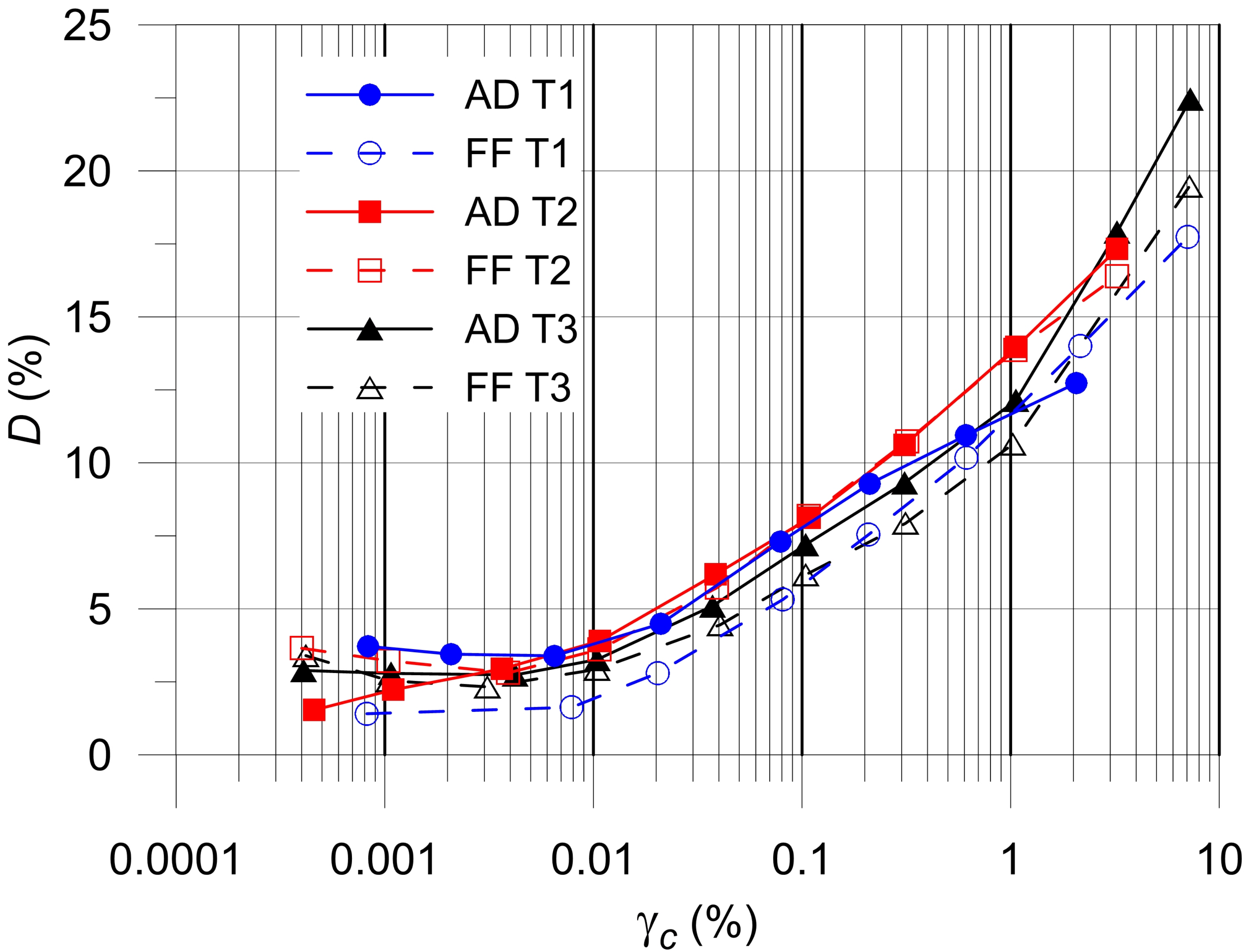

AD T1
FF T1
AD T2
FF T2
AD T3
FF T3
25
20
15
10
5
0
D (%)
0.0001
0.001
0.01
0.1
1
10
γc (%)

Table 1. Sample quality assessed on the basis of Δe / e_0 and M_0 / M_L values from oedometer tests

Quality rating	Δe /e_0 for OCR 1–2	Ratio M_0/M_L
Very good to excellent (1)	< 0.04	> 2.0
Good to fair (2)	0.04–0.07	1.5–2.0
Poor (3)	0.07 – 0.14	1.0 –1.5
Very poor (4)	> 0.14	<1.0

Table 2 Summary of results and setup data for the six corings (After Magagnoli, 2016)

Coring	Wather depth (m)	Barrel length (m)	Free fall (m)	Slack (m)	Head mass (Mg)	Penetration (m)	Recovery (m)	Recovery (%)
A-AD	673	15	0	0	1.55	7.52	7.52	100
A-FF	»	»	2.5	3.40	»	9.95	9.43	94.8
B2-AD	260	10	0	0	1.55	4.30	4.17	97.0
B2-FF	»	15	3.0	2.80	»	11.03	9.00	81.6
B3-AD	240	10	0	0	1.85	5.30	5.15	97.2
B3-FF	»	15	3.5	4.25	1.55	10.20	7.26	71.2

Table 3 Summary of physical properties of the specimens subject to oedometer and cyclic shear tests

Specimen	Depth (m)	γ (kN/m^3)	w_n (%)	e_0	Clay-silt-sand fractions (%)	I_P, w_L	σ'_{v0} (kPa)	p'_c (kPa)	$\Delta e/e_0$	M_0/M_L
AD-1-ILOC	1.55	15.18	93.6	2.381	29-54-17		9	100	0.0802	1.87
FF-1-ILOC	1.15	15.33	87.8	2.246	17-50-33		9	50	0.084	0.30
AD T1	2.00	15.20	71.2	2.0	33-56-11	36, 71				
FF T1	1.55	15.50	67.6	1.79						
AD-6-CRS	2.15	15.62	72.3	1.945	36-56-8	26, 56	12.3	160	0.038	1.91
FF-6-CRS	1.75	15.43	68.6	1.848	39-53-8	25, 54	12.3	70	0.096	1.26
AD T2	2.85	16.10	65.5	1.92	38-54-8	27, 54				
FF T2	2.35	15.70	68.3	1.73	39-52-9	27, 58				
AD-2-ILOC	3.25	15.12	76.5	2.095	7-24-69*	26, 47	18	75	0.0525	4.03
FF-2-ILOC	2.65	16.28	80.0	1.930	9-65-26*	27, 46	18	60	0.080	1.19
AD T3	5.15	15.50	77.0.	1.73	31-63-6					
FF T3	4.05	15.10	74.0	1.70	27-67-6	25, 51				
AD-3-ILOC	5.75	16.21	80.0	1.942	10-56-34*	25, 47	33	60	0.0731	1.17
FF-3-ILOC	4.50	16.23	78.4	1.912	9-65-26*	24, 48	33	80	0.107	2.27
AD-4-ILOC	5.75	15.94	83.1	2.045	10-50-40*	26,51	33	90	0.0465	1.88
FF-4-ILOC	4.50	15.75	80.2	2.033	10-64-26*	27, 51	33	90	0.064	1.04

* Grain size composition of coarser layers bounding the specimen

Table 4 Summary of testing conditions of specimens subjected to DSDSS tests

Specimen	Depth (m)	γ_c (%)	σ'_v(kPa)
AD T1	2.00	0.0008 - 2	12,0
FF T1	1.55	0.0008 - 7	
AD T2	2.85	0.0005 - 7	14.5
FF T2	2.35	0.0004 - 7	
AD T3	5.15	0.0004 - 7	27.8
FF T3	4.05	0.0004 - 7	

Table 5. Cyclic properties at low strains and initial void ratio of the tested specimens

	Depth (m)	e_0	G_0 (MPa)	D_0 (%)
AD T1	2	2.0	2.2	3.7
FF T1	1.55	1.79	1.9	1.4
AD T2	2.85	1.92	2.6	2.0
FF T2	2.35	1.73	2.3	3.0
AD T3	5.15	1.73	4.6	2.8
FF T3	4.05	1.70	4.0	2.5